Ageing of Silicone Rubber Composite Insulators on 400 kV Transmission Lines

IEEE Trans DEI 14 Issue 1 (2007) 130-136

S M Rowland, Y Xiong, J Robertson, S Hoffman

DOI: 10.1109/TDEI.2007.302881

Aging of Silicone Rubber Composite Insulators on 400 kV Transmission Lines

S. M. Rowland, Y. Xiong, J. Robertson
The School of Electrical and Electronic Engineering,
The University of Manchester,
PO Box 88, Manchester, M60 1QD, UK

and **S. Hoffmann**
National Grid,
Warwick Technology Park,
Gallows Hill, Warwick, CV34 6DA, UK

ABSTRACT

A number of silicone rubber composite insulators have been examined following 15 years of service on a coastal 400 kV transmission line in the UK. Extensive measurements of their hydrophobicity, as determined by contact angle, are given along with a description of their appearance. The hydrophobicity change varied from the low voltage end to the high voltage end with the lowest contact angles being found in the middle of the string. The sheds also aged differently around their circumference and this was reflected in discoloration differences on different sides of the insulator, in addition to hydrophobicity changes. The greatest change to properties was witnessed on the core of the insulators on which contact angles of less than 70 degrees were recorded.

Index Terms — S**ilicone rubber, composite, insulators, hydrophobicity, contact angle, aging, transmission line, NCI.**

1 INTRODUCTION

COMPOSITE overhead line insulators have been used over the last twenty years and are becoming more widespread. Originally they were deployed on low voltage systems, but their application has gradually become more accepted on higher voltage transmission networks. Composite insulators consist of pultruded glass-reinforced composite cores, which are protected by a polymeric sheath and sheds. The ends of the insulators are terminated by metallic fittings which are mechanically fastened to the pultrusion, and sealed to the polymeric sheath in a variety of proprietary ways [1].

Two principal mechanisms exist for failure of overhead line polymeric insulators. These are mechanical failure and electrical flashover. Mechanical failure is catastrophic and irreversible. Early insulators suffered from this mode of failure, often due to poor sealing between the end fittings and the polymer allowing water ingress. Modern designs have overcome this problem and the challenge in this area is now one of quality control [2,3]. However, moisture ingress can still occur if electric discharges erode sufficient sheath material. This is a key mode of failure due to long-term electrical activity, but results in mechanical failure through stress corrosion of the glass-reinforced strength member [3].

Electrical flashover can result from transients on the network or a reduction in an insulator's withstand capability below working stresses. The insulator recovers from an electrical flashover, but such an occurrence at working stresses must be seen as a system failure. An insulator prone to such an event is considered as 'failed' and has to be serviced or replaced. The circumstances for this are likely to be in high pollution conditions, after a prolonged period of ageing.

The ageing mechanisms and flashover processes are different for traditional ceramic systems and composite insulators. This is mainly due to the higher hydrophobicity of the polymeric surfaces of composite systems and the different ageing characteristics [4-6]. This is particularly true for silicone rubber. There remains a need to clarify these ageing processes for composite systems because many of the testing and type approval techniques presently employed have been derived from long experience with the ceramic materials, and are not directly applicable to the more recent materials.

Despite the complexity of the ageing chemistry of the silicone rubber materials under consideration, it is hydrophobicity which is key to the wet performance of the material. This is because when the material is highly hydrophobic, water molecules form discrete droplets on the

Manuscript received on 20 March 2006, in final form 7 August 2006.

surface of the insulation with high contact angles. As the polymeric material becomes aged, the degree of hydrophobicity is decreased and the material becomes more hydrophilic in nature. Under these conditions water then forms droplets with low contact angles. Under the influence of high electric fields these water droplets can proceed to form layers or elongated fingers of water, which can lead to the flow of currents over the surface of the insulation [7]. The flow of substantive currents may then lead to greater intensity of arcing, further material damage and even flashover events [8].

Failures of such insulators are not frequent, and since they have not been in use long, there is limited field experience. This paper presents hydrophobicity measurements from insulator surfaces which have been removed after 15 years' service on a 400 kV transmission line in the UK.

2 INSTALLATION SITE AND HISTORY

The insulators reviewed were in service on a 400 kV overhead transmission line as part of a National Grid pilot scheme. All the insulators were employed as suspension assemblies and had corona/stress-relief rings fitted. Conditions are reasonably aggressive due to the proximity of the line to the south coast of England, with prevailing south west winds and high salt and moisture levels in the air. The line follows the side of a hill approximately 10 miles from the Plymouth coast, which allows exposure to the elements on the south side of the insulators, whilst the north side is given some protection by the side of the valley. Since the region is agricultural, with minimal industrial activity, the proximity to the coastline suggests the main source of pollution is through salt spray. The line lies approximately 50º N, 5º W.

The climate varies by the hour and over distances of kms in this region, however, the following gives information about average climate over the last 30 years [9,10]. The wettest month is December which sees an average monthly precipitation of 125 mm. July is the driest month with 45 mm of rain. Records show least sunshine in December with a monthly average of 56 h and most in July at 228 h. The monthly average wind speed is fairly uniform throughout the year at around 12 knots, predominantly from the South West (and the Atlantic Ocean). The mean wind speeds are greatest in January at 14 knots, and least in July at 10 knots. The greatest wind speeds are seen when the wind is from the Atlantic. The average maximum temperature in August is 19 ºC, and temperatures above 30 ºC are unusual. The average minimum temperature in August is 12 ºC. Ground frosts can occur between October and May. An average of 13 days of air frost is seen over the winter. There are on average fewer than 10 days with snowfall each winter and 1 day with lying snow each year.

Eighteen silicone rubber composite insulators were installed, one per tower on an existing line over 7 km. The insulators have not shown any signs of imminent failure, such as high flashover statistics or physical cracking of the sheds.

Table 1. 400 kV Insulator Details.

Item	mm
Core Diameter	30
Shed Diameter	148
Number of Sheds	72
Creepage Distance	10230
Length of Insulator	3050
Distance Between Sheds	60

Other composite insulators examined on this line over the duration of this trial did not fare so well, and were replaced previously. The insulators reported here were removed on a routine refurbishment program 15 years after installation.

Each insulator consists of 72 identical silicone rubber sheds assembled on a core of 120 kN tensile strength. The overall length of the insulator is 3.35 m, with a creepage distance of 10.23 m. This provides a creepage distance to electrical stress ratio of 25.6 mm/kV, which corresponds to a 'high' contamination classification as defined by Looms [1]. The construction parameters of the insulators are given in Table 1.

3 CONTACT ANGLE MEASUREMENTS

One of the characteristics of silicone rubber insulators is that they have the ability to recover a degree of their hydrophobicity once removed from the ageing factors. For this reason the delay between the observations and removal from service is important. It is normally considered that a material's 'recovery' requires less than 12 hours [11,12]. These measurements were made many days or even months after removal from service. Thus the surfaces of the insulators had time to fully 'recover' from short-term ageing effects before the contact angles were determined.

Contact angles were measured at the locations indicated in Figure 1. For these measurements the insulator was oriented so the surface under consideration was approximately horizontal: for the core (position A) the string was horizontal, for the top surface (position B) the string was vertical, for the bottom surface (positions C and D) the string was upside-down. The water droplets were placed by a syringe onto the surface under study. The contact angle was recorded with a digital camera and the data analysed by software. Pictures of high and low contact angles are shown in Figure 2.

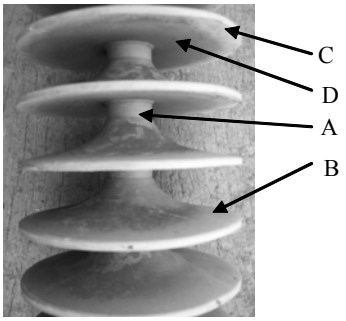

Figure 1. A typical composite insulator showing positions at which contact angles were measured.

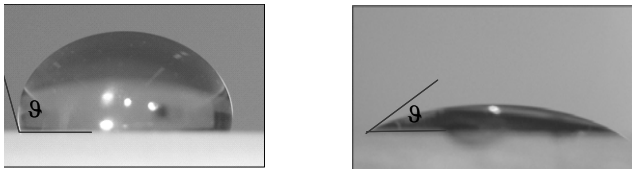

(a) high contact angle (b) low contact angle

Figure 2. Two extreme examples of contact angles.

4 RESULTS

4.1 VISUAL OBSERVATIONS

Although each insulator string removed from service was somewhat different, it is useful to produce a stereotype, which illustrates the visible features most frequently seen. Most had some or all of the following features to varying degree:

- Grey/brown deposits on the tops and undersides of sheds; these were heavier toward the HV, bottom end of the insulator, and on the north side
- No evident deposits on the top surface of the south side of the sheds but the polymeric material was bleached white
- A white residue on the core between the sheds
- Small amounts of green algae sometimes grew on the north side of the insulators, and this was heavier in the middle of the string

In a few cases insulators also showed:

- A whitening on the underside at the edge of each shed (i.e. the rim)
- Some slight surface crazing at the top surface on the edge of a shed

Insulators also occasionally showed typical signs of service contamination such as guano and tower-paint splashes.

In general, visual observations on site revealed the discolored material to be hydrophilic with a contact angle of less than 90 degrees and sheens of water forming, whereas the material with brown or green deposits was found to be more hydrophobic with a greater contact angle and water readily forming droplets. Figure 3 illustrates the difference in water drop formation on the south and north facing sides of the insulator: 3a) shows large continuous areas of water being formed, whereas distinct small droplets are evident in 3b).

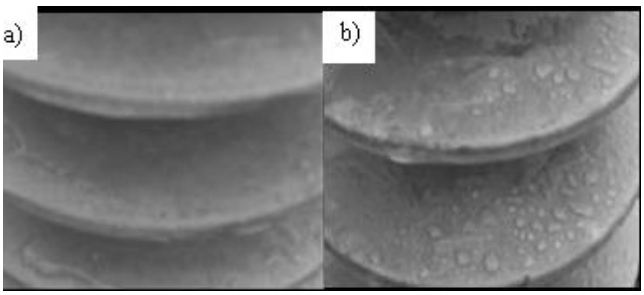

Figure 3. Illustrations of water droplet formation on the: a) hydrophilic south side and b) hydrophobic north side of the insulator.

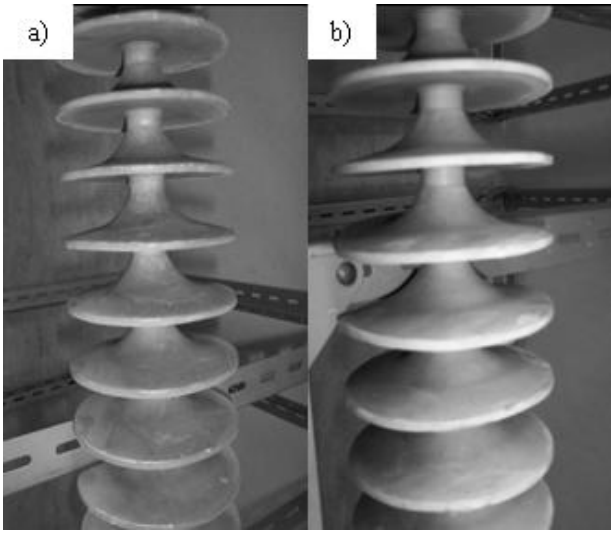

Figure 4. Two photographs of the same insulator: a) the dirtier north-facing side, b) the bleached south-facing aspect. The white rim can be seen on the underside of the sheds in the top of both of the pictures.

To illustrate the changes in color, Figure 4a shows the accumulated algae which was present on the sides of the sheds facing the hills of the valley, and Figure 4b shows discoloration on the side of sheds which have been exposed to the sun. Figure 5 identifies a particularly dirty set of sheds with crazing of the surface of the silicone rubber. The very light edges on the sheds to the front of the picture are due to the process of removal from the tower; effectively these areas have been scraped clean.

It appears from visual inspection that the two greatest changes to the insulator are the discoloration on the south side top surface of the strings and the dark deposits witnessed on the north-facing high voltage end of the string.

Figure 5. Dirty sheds. Nearest the camera are regions of crazed surface. The light areas at the very front were probably cleaned off during removal of the insulator from the tower.

4.2 CONTACT ANGLE MEASUREMENT

Contact angle investigations were carried out on a total of 18 strings. Measurements were made on 11 of the 72 sheds evenly distributed along the strings. For each shed, measurements were made on surfaces facing north, east, south and west, on the top and bottom surfaces of the sheds and also along the insulator core. The contact angles corresponding to the same location on each insulator have been averaged to show the trend of hydrophobicity along the whole string. Tables 2 to 5 give the contact angle averaged over the 18 measurements for the various locations A to D (as defined in Figure 1) and the associated standard deviation. The first column identifies the shed number counted from the top. Errors in angle measurements are estimated at $\pm$2%. It can be seen that natural variation is greater than this value. Figures 6 to 9 show the average contact angle for each of the four compass directions, at each of the locations. The equivalent tabulated and graphical data are adjacent to each other on the page for convenience of the reader. Also shown on the figures are the lines of best fit as given by Excel's second-order polynomial function. To avoid too much clutter on the graphs, the spread of results is illustrated in Figures 6 to 9 by an arrow on each of the north side and south side data. These arrows represent the average standard deviation for all the sheds in that location and face.

Figure 10 shows the typical spread of results on the core in more detail by illustrating the maximum and minimum values recorded on the north and south faces. It can be seen that the spread of results can be significant and small changes in average values of a few degrees do not imply consistency between every insulator, and may not imply a real difference. Nonetheless the case displayed here shows the difference between the north and south core faces is substantial, the maximum contact angle on the south core face being similar to the minimum seen on the north face for the 18 insulators measured. The two faces become indistinguishable at the high voltage end where the contact angles are greater and ageing less pronounced.

Measurements made on unaged material of the same composition as the installed insulators gave an average contact angle measurement of 103 degrees with a standard deviation of 1.0 degree.

5 DISCUSSION

The contact angle measurements show considerable variation from top to bottom of the insulator, circumferentially through the compass directions, and also with the orientation of the particular surface being considered. Generally Figures 6 and 9, showing results on the core and the inner bottom surface, are similar to each other. Figures 7 and 8, showing data form the top and rim, are also similar to each other. Each is considered below before general observations are made.

That the standard deviation of the measurements on new material is much lower than that on aged material suggests that the scatter in results seen is due to variation between samples rather than experimental error.

5.1 VARIATION ALONG THE LENGTH

The insulators were installed with corona rings at both ends, which will have reduced the stress at the very top and bottom of the string. This may explain the extreme 'bath tub' shape of the curves seen in Figures 6 and 9. Also the top of the uppermost shed, the underside of the bottom shed and the core below it are more exposed to wind, salt spray and the natural elements. In particular, the uppermost shed will see more direct sunlight than the rest of the insulator. It may be for these reasons that the core has a particularly high contact angle at the top and bottom of the strings as shown in Figure 6. This is not reflected in a similarly high value on the top surface of the top shed in Figure 7, perhaps due to the impact of sunlight. However, the inner, underside of the bottom insulator does appear to reflect this effect in Figure 9.

The hydrophobicity of the sheds tends to a minimum in the centre of the string rather than at the HV end. This is particularly true for the core measurements. The top surface measurements presented in Figure 7 suggest minimal variation along the length, with the exception of the south side which appears more aged at the top LV end. Previously a strong decrease in hydrophobicity has been reported toward the HV end on EPDM [13] and silicone materials [14,15], although such a dependency is not always observed [16,17,18].

5.2 CIRCUMFERENTIAL VARIATION

The contact angles measured on both the top and bottom surfaces of the sheds were higher on the north side than on the exposed south side where material was discolored. Thus the insulator shed surfaces are more hydrophobic on the north side than on the exposed south side. This suggests that the natural environment plays a large part in the ageing process. A similar effect has previously been reported on EPDM insulators aged in service [13].

The variation between the north face and the south face is always more pronounced (by several degrees) on the top surface rather than underneath. In the centre of the string on the underside, the variation is not so great. This illustrates the importance of solar radiation on the ageing process. The greatest difference between north and south is seen on the core in the center of the insulator length; the reason for this is not so clear, but may be due to enhanced electrical activity in this region.

There is very little evidence in the literature for circumferential variation of properties after ageing. It has, however, been noted in an installation in China that on the side of the prevailing wind, greater ageing took place. This was ascribed to heavier pollution deposits rather than a change in moisture deposition or drying, and no relationship to the direction of the sun was reported [19,20].

5.3 SHED AND CORE SURFACE VARIATION

The contact angle measurements on the bottom surfaces of sheds near the insulator core, shown in Figure 9, are similar in magnitude and behavior to those on the insulator core, in Figure 6, on the north side. However, there are significant

Table 2. Mean contact angles and standard deviations on the core.

No.	North		East		South		West	
	Angle	S.D.	Angle	S.D.	Angle	S.D.	Angle	S.D.
0	102	3.7	102	4.4	99	2.7	104	2.7
7	95	2.7	93	3.5	86	5.9	90	3.5
14	96	2.7	93	6.6	86	6.7	91	4.8
21	94	2.5	88	5.7	83	7.1	89	5.1
28	95	2.3	86	6.5	82	6.4	88	4.5
35	93	2.0	87	3.7	83	4.9	87	3.6
42	93	2.1	88	2.4	84	2.9	90	2.3
50	96	2.7	92	2.2	83	5.1	91	1.9
57	96	3.8	94	3.7	89	5.0	93	1.7
64	97	2.0	94	2.5	93	2.7	95	1.6
72	103	3.2	103	3.2	103	1.8	104	3.2

Table 3. Mean contact angles and standard deviations on the top surface.

No.	North		East		South		West	
	Angle	S.D.	Angle	S.D.	Angle	S.D.	Angle	S.D.
0	94	3.7	90	1.7	89	2.1	94	5.8
7	97	1.7	90	1.5	90	3.3	93	1.8
14	95	3.1	89	5.4	92	2.3	92	1.4
21	94	3.9	93	5.1	88	4.5	91	2.1
28	93	4.7	89	3.1	90	3.4	93	3.7
35	95	5.0	92	2.2	86	6.9	91	1.1
42	94	3.9	91	3.2	88	3.0	91	3.3
50	97	4.5	90	2.5	86	3.5	92	1.5
57	97	5.6	91	1.7	88	4.1	89	3.6
64	95	4.4	91	1.6	86	3.4	93	3.7
72	99	3.7	93	1.5	89	4.7	94	3.3

Table 4. Mean contact angles and standard deviations on the outer underside.

No.	North		East		South		West	
	Angle	S.D.	Angle	S.D.	Angle	S.D.	Angle	S.D.
0	93	1.6	95	5.1	91	1.5	90	0.7
7	94	2.6	91	2.2	90	2.0	92	1.2
14	91	2.8	91	2.8	87	2.5	91	1.0
21	92	0.9	92	1.9	88	3.3	91	0.9
28	92	2.0	91	3.7	89	2.2	91	2.5
35	92	2.9	91	2.3	88	4.2	92	1.6
42	92	1.8	91	1.5	89	4.2	92	1.9
50	94	3.1	92	1.7	90	3.7	92	1.7
57	97	4.7	93	1.9	91	2.2	92	1.8
64	99	5.7	93	2.9	90	1.8	93	1.7
72	101	6.3	98	3.8	94	5.0	95	2.6

Table 5. Mean contact angles and standard deviations on the inner underside.

No.	North		East		South		West	
	Angle	S.D.	Angle	S.D.	Angle	S.D.	Angle	S.D.
0	101	3.7	99	4.9	91	1.8	94	5.2
7	97	3.6	94	2.8	92	3.0	92	3.0
14	93	2.7	95	2.5	90	4.7	93	2.3
21	93	2.2	94	2.4	91	2.3	93	1.3
28	94	3.1	91	3.8	92	3.4	94	3.0
35	95	1.9	93	2.6	90	5.0	94	1.3
42	96	1.8	94	2.5	91	5.3	93	1.4
50	96	4.2	95	1.5	92	3.1	94	2.0
57	98	4.0	97	4.4	94	3.0	94	3.6
64	101	4.7	95	1.9	96	4.3	96	4.9
72	102	4.0	100	3.6	97	6.0	100	4.8

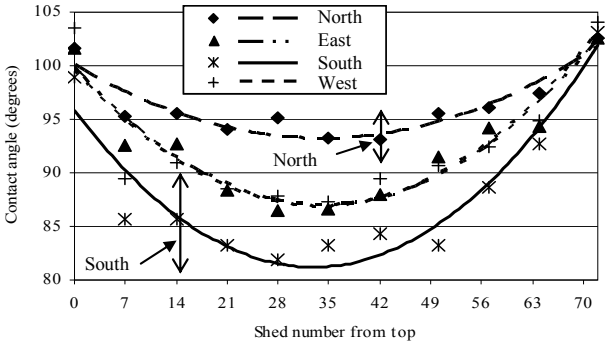

Figure 6. Average contact angle along the core of each insulator in each of the compass directions (position A, Figure 1).

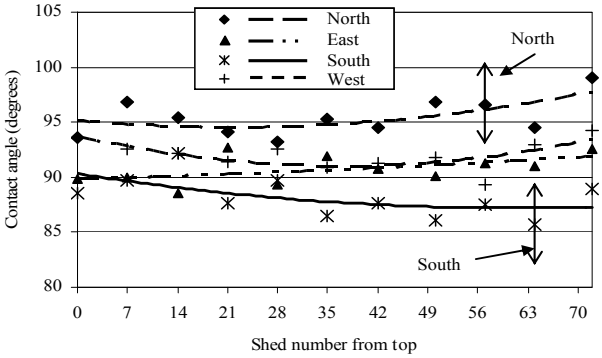

Figure 7. Average contact angle on the top surface of the sheds in each of the compass directions (position B, Figure 1).

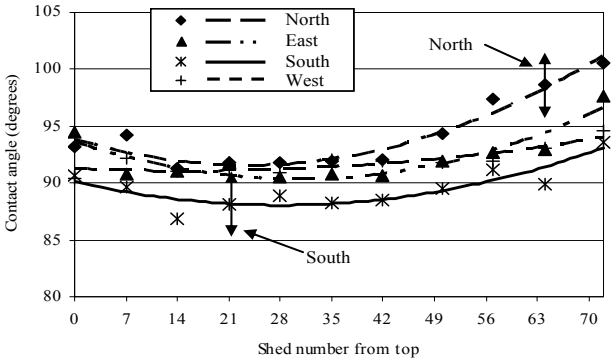

Figure 8. Average contact angle distribution on the outer edge of the bottom surface of the sheds in each of the compass directions (position C, Figure 1).

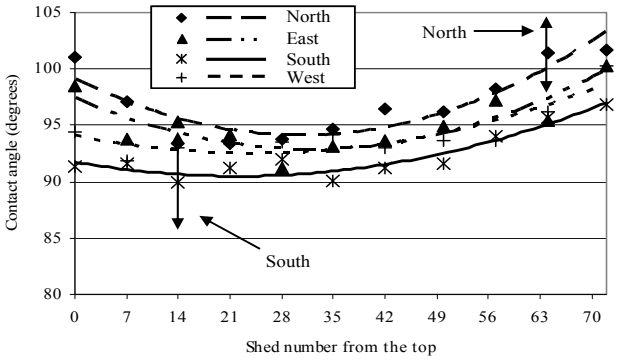

Figure 9. Average contact angle distribution on the inner bottom surface of the sheds down the string in each compass direction, (position D, Figure 1).

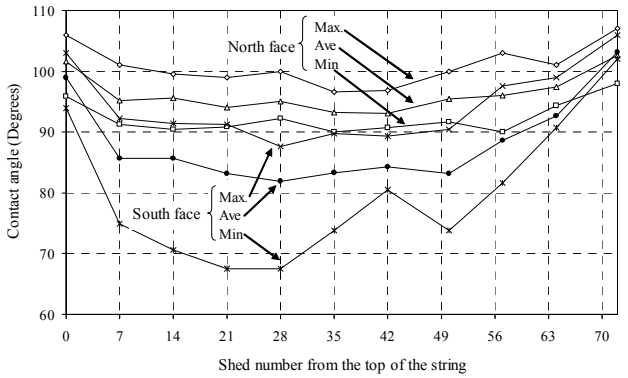

Figure 10. An example of the spread of data between the 18 insulators. The maximum and minimum of the contact angles for two faces of the core is shown for the 18 insulators examined.

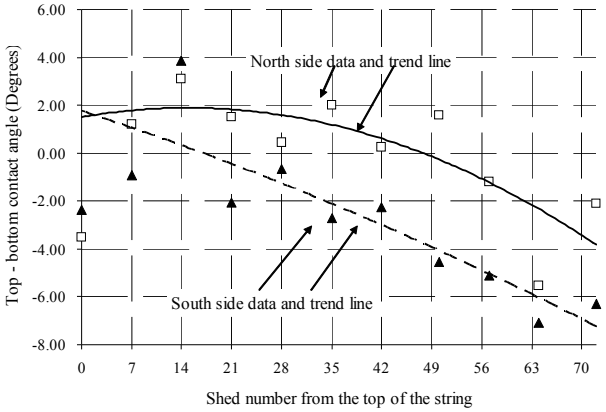

Figure 11. The difference between the contact angle on the top face and the average of the two lower-surface measurements.

differences on the other sides, and particularly low values on the south side on the core. The variation between the top and bottom surfaces of the sheds is marked. The average measurements from the top of the sheds is more consistent from top to bottom of the string, varying only six degrees on each face. However, on the core the variation is up to twenty degrees from the HV to the LV end, with the lowest values in the centre. This suggests that parts of the core are more heavily damaged than the sheds. One explanation for this is that this part of the insulator presents a smaller cross-section to leakage currents, which results in a higher current density, and so a higher likelihood of discharges and dry-band arcing than on the sheds. Also, in this region the electric field is parallel to the insulator surface, promoting surface discharges.

The difference between the top and bottom surfaces of the sheds is illustrated in Figure 11. Here the difference between the contact angle on the top surface and the average of the two bottom surface locations is produced for the north and south sides. It can be seen that on the north-facing surface, the average contact angle is greater on the top face and so the hydrophobicity is greatest on the top side. Towards the HV end, however, the trend is reversed and the sheds' undersides tend to be less aged that the tops. On the south side it is generally the case that the top surface is more aged than the bottom side. Second-order polynomial lines of best fit are shown on the Figure. The data points at the very top of the insulator have been disregarded in generating these curves. The line is almost a linear fit for the south side, and represents a good fit at the HV end.

Differences have been reported previously in hydrophobicity on the top and bottom side of aged shed surfaces. Normally the contact angle is smaller on the underside of the shed than the top side [16,17,18].

5.4 ENVIRONMENT AND HYDROPHOBICITY

From the results above, it is evident that the regions of the sheds (on the south side) which have been most exposed to the sun have discolored and are most hydrophilic in nature. Since the area where the towers are installed is rural, with no signs of heavy industry (or acid rain), it is suggested that this effect is predominantly due to exposure to UV radiation. The cause of discoloration/white rings at the edges of the bottom surface on some of the sheds is unclear. This discoloration was not always present and so further work is required to understand the cause, although such discoloration is indicative of discharge activity.

The north side of the insulators showed both a high hydrophobicity and the presence of algae. From these observations it may be suggested that the presence of the algae promoted hydrophobicity. This may also explain the high contact angles at both the top and bottom sheds on the insulator strings, since there was also a high concentration of algae in these regions. One complication to this argument is that the insulators have been stored indoors in a dry environment since decommissioning, and algae may have died in that period. Investigations into the effects of fresh algae are required to determine whether this further influences the hydrophobicity. It may also be that in service, the presence of algae provides shade to the underlying material, thereby preventing damage by solar radiation. The dielectric properties of any such surface layer are also likely to modify local fields. Algae is less often observed on the south side of the string. This could be due to the natural wetting and drying of rain water. Due to the topology of the line, rain water is predominantly directed from the south, and washed to the north face. Similarly, wind and sun would tend to dry the south side first, allowing better growing conditions on the north side, as seen on tree trunks. Once algae is present, it will tend to hold moisture on the surface longer and further promote algae growth on the north side.

The insulator core would not have seen direct effects of sunlight and UV radiation, due to the shading effect of the sheds. Nonetheless the insulator core facing the south has the lowest contact angles. However, despite the reduced contact angles there is little sign of discoloration of the polymer insulation in this region, although there is some evidence of white residue. It is therefore suggested that the ageing of the insulator core is primarily due to surface discharge activities.

Surface discharges on the core may be due to the decreased hydrophobicity on the south-facing top surface of the insulator sheds. Conduction over the surface of the insulator in this region would then intensify the field distribution on the insulator core, giving an increase in the probability of aging of the core through water droplet corona and dry-band arcing. That the lowest contact angles measured are on the core facing the sun (the south side), may be because light is still more intense on the shaded south side than the north, or it may be because discharge activity is most active at the south side of the core. The low contact angles on the south side of the insulator suggest that leakage current will predominantly flow on that side of the insulator and so preferentially promote further discharges on that side.

The complex geometry and discrete nature of water droplets has been the focus of much modeling of electrical fields so that levels of surface discharge activity can be predicted and understood [21,22]. These are complex calculations, but it is clear that the non-uniform nature of an aged polymeric insulator's surface also needs to be considered if a complete picture is to be derived. In particular the evolving end-to-end variation and reduced rotational symmetry need exploration.

6 CONCLUSIONS

Measurements of hydrophobicity and visual observations of the surface of field-aged 400 kV silicone rubber composite insulators show variations from end to end and circumferentially. On one string the contact angle varied between 82 and 104 degrees. Within one insulator shed the contact angle varied 11 degrees across its face from north to south. The side of the insulator which faced the sun and prevailing winds from the sea aged faster, as measured by loss of color and reduced contact angle with water. That side of the insulator was also the only one whose top surface had a lower contact angle than its bottom surface.

The part of the insulator which showed the lowest contact angle was the south-facing core in the centre of the string. It is suggested that this, and the white deposits seen on the polymer surface, are indicative of discharge activity in this region.

Even in mild UK climate the prevailing climate has been shown to have a major impact on the ageing of insulators. Detailed chemical analysis is required from many faces of an insulator to generate a complete picture of the ageing processes. Electric field analysis models need also to account for the lack of rotational symmetry of the system, and end-to-end variation of surface properties.

ACKNOWLEDGMENT

The authors are grateful to National Grid for the support of this research, and for their permission to publish.

REFERENCES

[1] J. S Looms, *Insulators for High Voltages,* Peter Perigrinus, 1988.
[2] J. Mackevich and M. Shah, "Polymer outdoor insulating materials. Part I: Comparison of porcelain and polymer electrical insulation", IEEE Electr. Insul. Mag., Vol. 13, No. 3, pp. 5-12, 1997.
[3] K. Kumosa, L. Kumosa, and D. Armentrout, "Failure analysis of non-ceramic insulators Part 1: Brittle Fracture Characteristics", IEEE Electr. Insul. Mag., Vol. 21, No. 3, pp.14-27, 2005.
[4] G. G. Karady, "Flashover mechanism of non-ceramic insulators", IEEE Trans. Dielectr. Electr. Insul., Vol. 6, pp. 718-723, 1999.
[5] A. J. Phillips, D. J. Childs and H. M. Schneider, "Water drop corona effects on full-scale 500 kV non-ceramic insulators", IEEE Trans. Power Del., Vol. 14, pp. 258-265, 1999.
[6] R. Hackam, "Outdoor HV composite polymeric insulators", IEEE Trans. Dielectr. Electr. Insul., Vol. 6, 557-585, 1999.
[7] G. G. Karady, M. Shah and R. L. Brown, "Flashover mechanism of silicone rubber insulators used for outdoor insulation-I", IEEE Trans. Power Del., Vol. 10, pp. 1965–1971, 1995.
[8] D. A. Swift, "Insulators for outdoor applications", Advances in High Voltage Engineering IEE Power and Energy Series Vol. 40, ed. A. Haddad, and D. Warne, 2004.
[9] www.bbc.co.uk/weather/world/city_guides.
[10] www.met−office.gov.uk/climate/uk/location/southwestengland/wind.html
[11] S. Simmons, M. Shah, J. Mackevich and R. J. Chang, "Polymer outdoor insulating materials. Part III-Silicone elastomer considerations", IEEE Electr. Insul. Mag., Vol. 13, No. 5, pp. 25-32, 1997.
[12] D. K. Bhana and D. A. Swift, "An investigation into the temporary loss of hydrophobicity of some polymeric insulators and coatings", IEEE 4th Int. Conf. on Properties and Applications of Dielectric Materials, Brisbane, Paper 5208, 1994.
[13] R. Sundararajan, N. Amohammed, T. Chaipanit, Z. Karcher and Z. Liu, "In-service aging and degradation of 345 kV EPDM transmission line insulators in a coastal environment", IEEE Trans. Dielectr. Electr. Insul., Vol. 11, pp. 248-361, 2004.
[14] D. Birtwhistle, P. Blackmore, A. Krivda, G. Cash and G. George, "Monitoring the condition of insulator shed materials in overhead line distribution networks", IEEE Trans. Dielectr. Electr. Insul., Vol. 6, pp. 612 – 619, 1999.
[15] H. Liu, G. Cash, D. Birtwihistle, and G. George, "Characterisation of a severely degraded silicone elastomer HV insulator – an aid to development of lifetime assessment techniques", IEEE Trans. Dielectr. Electr. Insul., Vol. 12, pp. 478-486, 2005.
[16] A. E. Vlasatos, and S. M. Gubanski, "Surface structural changes of naturally aged silicone and EPDM composite insulators", IEEE Trans. on Power Del., Vol. 6, pp. 888-890, 1991.
[17] S. M. Gubanski and A. E. Vlasatos, "Wettability of naturally aged silicone and EPDM composite insulators", IEEE Trans. on Power Del., Vol. 5, pp. 1527-1535, 1990.
[18] A. E. Vlastos and E. Sharif, "Natural ageing of EPDM composite insulators", IEEE Trans. Power Del., Vol. 5, pp. 406-410, 1990.
[19] S. Wang, L. Xidong and G. Zhicheng, "Investigation on hydrophobicity and pollution status of composite insulators in contaminated areas", IEEE Conf. Electr. Insul. Dielectr. Phenomena (CEIDP), pp. 628-631, 2001.
[20] Z. Cheng, L. Xidong, Y. Wang, X. Wang, Y. Zhou and Z. Li, "Investigation on composite insulators in contaminated areas", IEEE Conf. Electr. Insul. Dielectr. Phenomena (CEIDP), pp. 327-330, 2002.
[21] W. Que and S. A. Sebo, "Typical cases of electric field and voltage distribution calculations along polymer insulators under various wet conditions", IEEE Conf. Electr. Insul. Dielectr. Phenomena (CEIDP), pp. 840-843, 2002.
[22] H. El-Kishky and R. S. Gorur, "Electric field computation on an insulating surface with discrete water droplets", IEEE Trans. Dielectr. Electr. Insul., Vol. 3, pp. 450-456, 1996.

Simon M. Rowland (M'05) was born in London, England. He completed the B.Sc. degree in Physics at UEA and his Ph.D. degree at London University. He was awarded the IEE Duddell Premium in 1994 and became a FIEE in 2000. He has worked for many years on dielectrics and their applications. He has also been Operations and Technical Director in a multinational manufacturing company. He joined The School of Electrical and Electronic Engineering in The University of Manchester as a Senior Lecturer in 2003.

Yu Xiong (M'05) was born in Nanning, China. He completed the B.Sc. degree in electrical engineering at Wuhan University in 1993 and the M.Sc. degree at UMIST in 2004. He has worked for some years on power system design. He is currently a Ph.D. student at the University of Manchester investigating the aging mechanisms of composite polymeric insulator systems.

Jeff Robertson (M'02) was born in Liverpool, England. He completed the B.Sc.-M.Eng. in electrical and electronic engineering in 2000, and has recently received his Eng.D. degree from the University of Manchester. He is currently working as a Research Associate at the University of Manchester, investigating the aging mechanisms of composite polymeric insulator systems. He is an active committee Member of the IEE.

Sven Hoffman was born in Stuttgart, Germany. He completed the B.Eng. degree in mechanical engineering at the University of Birmingham in 1995. He is currently the Forward Policy Team Leader (Circuits and Pipelines) at National Grid in Warwick, having worked with overhead lines for many years. He is a Chartered Engineer with the IEE, and the UK Regular Member of CIGRE Study Committee B2.